

**RESEARCH ARTICLE**

# The effect of manufacturing method; direct compression, hot-melt extrusion, and 3D printing on polymer stability and drug release from polyethylene oxide tablets

**Nour Nashed<sup>1</sup>**, **Barnaby W. Greenland<sup>1</sup>**, **Mridul Majumder<sup>2</sup>**, **Matthew Lam<sup>1,3</sup>**, **Taravat Ghafourian<sup>4</sup>**, and **Ali Nokhodchi<sup>1,5\*</sup>**

<sup>1</sup> Arundel Building, School of Life Sciences, University of Sussex, Brighton, United Kingdom

<sup>2</sup> M2M Pharmaceuticals Ltd., Reading, United Kingdom

<sup>3</sup> Department of Chemical and Pharmaceutical Sciences, School of Human Sciences, London Metropolitan University, London, United Kingdom

<sup>4</sup> Barry and Judy Silverman College of Pharmacy, Nova Southeastern University, Ft. Lauderdale, Florida, United States of America

<sup>5</sup> Lupin Research Inc., Coral Spring, Florida, United States of America

## Abstract

Thermal 3D printing has gained substantial attention in pharmaceutical formulation, especially concerning its potential use in personalized dose delivery. The choice of a printable polymer is crucial in this technique, but it is restricted due to technical issues such as thermal stability and thermal-rheological properties of the polymers. Polyethylene oxide (PEO) is a widely used polymer in drug formulation designs, with potential application in 3D printing due to its favorable rheological properties. However, the thermal stability of PEOs exposed to high temperatures during fused deposition modeling (FDM) needs to be characterized. This research focused on the characterization of two molecular weights ( $M_w$ ) of PEO (7 and 0.9 M) under various manufacturing methods and formulation compositions. PEO was mixed with other low-viscosity polymers of hydroxypropyl cellulose (HPC) or ethyl cellulose (EC) to achieve printable formulations (PEO/HPC or PEO/EC). Tablets were manufactured by direct compression, compression of hot-melt extrudates (HME) at 150°, or by FDM 3D-printing at 220°. Differential scanning calorimetry (DSC), X-ray powder diffraction (XRPD), gel permeation chromatography (GPC), dissolution tests, and their kinetics studies were carried out. Results demonstrated that thermal processes could reduce the crystallinity of PEO and induce  $M_w$  reduction that varies depending on the  $M_w$  of PEO. As a result, dissolution efficiency (DE%) varied based on the formulation composition and manufacturing method. For formulations containing PEO and HPC, 3D-printed and HME tablets exhibited higher DE (>60%) compared to directly compressed tablets (DE < 50%), while for those with PEO and EC, 3D printing reduced DE% to <26% compared to direct compression (~30%) and HME tablets (~50%). This was attributed to the hydrophobic nature of EC and the increased hardness of the printed tablets, preventing tablet disintegration during dissolution, which outweighs the  $M_w$  reduction in PEO.

**Keywords:** Manufacturing method; Hot-melt extrusion; Polyethylene oxide; 3D printing; Molecular weight; Thermal stability

**\*Corresponding author:**

Ali Nokhodchi  
(a.nokhodchi@sussex.ac.uk)

**Citation:** Nashed N, Greenland BW, Majumder M, Lam M, Ghafourian T, Nokhodchi A. The effect of manufacturing method; direct compression, hot-melt extrusion, and 3D printing on polymer stability and drug release from polyethylene oxide tablets. *Int J Bioprint.* 2024;10(5):4055. doi: 10.36922/ijb.4055

**Received:** June 27, 2024

**Revised:** July 31, 2024

**Accepted:** August 2, 2024

**Published Online:** August 5, 2024

**Copyright:** © 2024 Author(s).

This is an Open Access article distributed under the terms of the Creative Commons Attribution License, permitting distribution, and reproduction in any medium, provided the original work is properly cited.

**Publisher's Note:** AccScience Publishing remains neutral with regard to jurisdictional claims in published maps and institutional affiliations.

## 1. Introduction

Polyethylene oxide (PEO) is a synthetic non-ionic hydrophilic polymer considered non-toxic in humans. It is readily available in a wide range of molecular weights ( $M_w$ ) up to 7 M. The  $M_w$  of the polymer used in the formulation can be selected to give a desired release profile with lower  $M_w$  typically used for rapid drug release since they dissolve quickly in water.<sup>1,2</sup> Conversely, the higher  $M_w$  PEOs (>0.3 M) are used in slow drug release systems.<sup>1,2</sup> In these instances, the PEO is known to swell in water, forming a hydrogel layer with increasing strength and thickness as  $M_w$  increases, thereby resulting in a slower drug release profile.<sup>3,4</sup>

Polyethylene oxide (PEO) degradation has been reported to occur at elevated temperatures in the presence of oxygen through a scission of the chemical bond between two carbon atoms, as well as the carbon-oxygen bonds, giving smaller fragments.<sup>5</sup> As a result, the  $M_w$  of PEO can decrease, which in turn reduces its viscosity.<sup>1,2</sup> Additionally, the crystallinity of PEO is dependent on its thermal history; specifically cooling rapidly from above its melting point ( $\sim 70^\circ$ ) can result in a low level of crystallinity in the product, which dramatically affects its solid-state properties.<sup>3,6</sup> This reduction in  $M_w$  and crystallinity during high-temperature processing, such as that encountered during hot melt extrusion (HME), is known to increase the drug release rates in formulated tablets.<sup>1,3,7</sup> Thus, it is challenging to maintain the desired extended-release behavior of high  $M_w$  PEO ( $\geq 0.9$  M) formulations when processed at elevated temperatures. Changes in  $M_w$  and crystallinity, and the resulting change in gelling behavior, are considered more pronounced when  $M_w$  of PEO is increased. For example, under the same storage conditions ( $40^\circ$ ), there was a more significant drop in the viscosity of PEO 7 M, hence a greater increase in drug release rate, compared to PEO 4 M.<sup>8,9</sup>

Based on thermogravimetric analysis (TGA) studies, Vrandečić et al. found that the degradation of PEO occurs within the temperature range of  $330\text{--}450^\circ$ , independent of its  $M_w$ . It was also noted that the heating rate had a mixed impact on degradation rates of low and high  $M_w$  PEOs; high  $M_w$  PEOs (1 and 5 M) degraded faster than low  $M_w$  PEOs (100 and 300 k) during rapid heating, while the pattern is inverse during slow heating rate.<sup>10</sup> Conversely, crystalline regions of PEO, which are more prevalent in high  $M_w$  PEO samples, appear to have better resistance to degradation than amorphous regions.<sup>10</sup> This may explain the lower stability of low  $M_w$  PEOs compared with high  $M_w$  PEOs.<sup>6,9</sup> Despite the aforementioned potential liabilities, PEO has been successfully processed by thermal methods (HME and injection molding [IM]) for drug delivery. For example, low  $M_w$  PEOs (<300 k) exhibit good stability under temperatures as high as  $140^\circ$  during IM,<sup>3</sup> consistent

with an earlier study of PEO for industrial applications where thermoplastic processing was recommended to be carried out at temperatures below  $130^\circ$ .<sup>11</sup>

In contrast, high  $M_w$  PEOs (>1 M) displayed a reduction in  $M_w$  when processed in a single screw extruder under elevated temperatures ( $100\text{--}170^\circ$ ) and short residence time (2–3 min).<sup>6,12</sup> In HME, PEO is subjected to both mechanical and thermal stresses;<sup>6</sup> thus, extruder configuration can impact the degradation process. In a recent study, formulations containing PEO (7 M) were processed in a twin screw extruder at  $130^\circ$ , which resulted in significant degradation, leading to reduced viscosity and accelerated drug release compared to unstressed formulations.<sup>1</sup> Accordingly, another study indicated that an increase in the  $M_w$  of PEO from 100 to 900 k delayed the drug release rate from HME extrudates as expected. Still, no significant extension in drug release time was achieved by further increasing the  $M_w$  from 0.9 M up to 7 M.<sup>13</sup> This can be interpreted as a sign of degradation of the high  $M_w$  PEO (0.9–7 M) during extrusion.

In practical terms, the high viscosity of molten high  $M_w$  PEO ( $\geq 0.9$  M) can hinder its printability in fused deposition modeling (FDM).<sup>14</sup> Thus, a mixture of high  $M_w$  PEOs with other polymers can be used to reduce the melt viscosity and facilitate its printability. In this case, flexible polymers, such as low  $M_w$  polyethylene glycol (PEG), can protect PEO during extrusion and printing.<sup>14,15</sup> Given the potential for PEO application in controlled-release drug formulation designs, its complicated behavior under high-temperature processing conditions, and the limited study on the  $M_w$  stability of 3D printed formulations containing PEO, the current study aimed to investigate (i) the impact of PEO  $M_w$  on its stability when mixed with other polymers; (ii) stability of PEO after dual thermal processing, i.e., HME followed by FDM printing of tablets; and (iii) the impact of PEO stability on physical properties and drug release from the manufactured tablets. Two  $M_w$  of PEO (0.9 and 7 M) were investigated under various processing conditions and in combination with hydroxypropyl cellulose (HPC) and ethyl cellulose (EC). Since theophylline is a thermostable drug, it was selected as the model drug for this study to minimize the effect of drug degradation on formulation characterization. Tablets from thermal processes, such as HME and FDM, were compared with milder, non-thermal processes, such as direct compression of a physical mixture of powders.

## 2. Materials and methods

### 2.1. Materials

Theophylline anhydrous (purity: >99%) was purchased from Fisher Scientific (United Kingdom, UK) and used as a model drug with a high melting point around  $273^\circ$ .

Low-viscosity HPC ( $M_w$ : ~95 k; Kucel™ EF) was provided by Ashland Inc. (Netherlands). Dibutyl sebacate (DBS) was supplied by Sigma-Aldrich (United States of America [USA]). EC ( $M_w$ : ~23 k, Ethocel 10 FP) and PEO ( $M_w$ : 7 M, POLYOX WSR 303; and  $M_w$ : 0.9 M, POLYOX WSR 1105) were obtained from Colorcon Ltd. (UK) as a gift.

## 2.2. Formulation development

Preliminary observation revealed that formulations solely containing PEO and theophylline were not printable because of the high melt viscosity of PEO ( $M_w$ : 0.9 and 7 M). Therefore, a mixture with other polymers was needed to produce printable PEO formulations (Table 1). Since the study focuses on the thermal stability of PEO, thermally stable polymers (HPC and EC)<sup>16</sup> were selected to be mixed with PEO. Theophylline percentage was kept constant (30% [w/w]) in all the developed formulations (see compositions in Table 1). In formulations containing EC (F<sub>3</sub> and F<sub>4</sub>), a plasticizer (DBS) was also added to improve printability and reduce the brittleness of EC. DBS was added to EC powder at 13% (w/w) of EC weight (equivalent to 5.2% of the total formulation), mixed thoroughly, and left overnight for better sorption of the liquid plasticizer to the EC chains. Thereafter, the plasticized EC was ready to use in making formulations F<sub>3</sub> and F<sub>4</sub>.

All studied formulations (F<sub>1</sub>–F<sub>4</sub>) were prepared into tablets by three distinct methods: direct compression of the physical mixture (PM), compression of HME extrudates, and 3D printing. All tablets were then studied for dissolution and other physical characteristics.

## 2.3. Tablet preparation

Tablets were prepared via three different methods: direct compression of PM, compression of powders prepared from HME, and 3D printing of HME filaments (via FDM). The manufactured tablets were stored in enclosed vials in a chamber at room temperature (22 ± 2°) and tested for dissolution within a week.

### 2.3.1. Physical mixture tablets

Using the formulation compositions mentioned in Table 1, the powders were mixed using mortar and pestle (approximately for 5 min). The powder blend was

compressed into a tablet of 333.3 mg with a hydraulic manual tableting press (Model MTCM-I; Globe Pharma, USA), equipped with 10 mm diameter concave punches. The employed pressure was 150 bar, and the dwell time was constant at 10 s.

### 2.3.2. Hot-melt extrudate tablets

The physical admixture was fed manually at (an average of) 1 g/min into a 10-mm twin-screw extruder L/D 20 (assembled by Point1 Controls/R Controls; Stoke-on-Trent, UK) at a screw speed of 50 rpm. The temperature of the feed zone was set at 130°, and the temperature for the rest of the zones (including the die) was set at 140°. Although this temperature exceeds the melting temperature ( $T_m$ ) of PEO (73°), it was necessary to exceed the glass transition temperature ( $T_g$ ) of HPC and EC mixed with PEO. Additionally, PEO was processed at high temperatures above its  $T_m$  to investigate (i) the impact of temperature and compare the results with other similar studies<sup>12,15,17</sup> and (ii) the effect of thermal process conditions on PEO stability and drug release. Filaments were collected manually using a winder. After collecting and cooling, the filaments were cut manually into small pieces around 2 mm in length using a pair of scissors. Then, 5 g of the resulting samples were transferred to a ball mill (PM 100; Retsch GmbH, Germany) and ground for 4 min at 400 rpm. The ground powders were collected from the ball mill and kept in tightly closed containers at room temperature. The powders were compressed into tablets using a hydraulic manual tableting press (Model MTCM-I; Globe Pharma, USA) equipped with 10 mm diameter concave punches. Compression was carried out at 150 bar with a 10-s dwell time. The nominal weight of each tablet was 333.3 mg, equivalent to 100 mg of theophylline.

### 2.3.3. Printed tablets

Filaments were prepared using HME, as mentioned earlier. The diameter of the filaments is crucial as the filaments should fit into the feeding nozzle of the FDM printer, which has a diameter of 1.75 mm. The diameter of the filaments was measured using a vernier caliper, and only filaments with a diameter ranging between 1.7 and 1.8

Table 1. Composition of studied formulations.

Formulation	Composition (%)					
	Theophylline	PEO (7 M)	PEO (0.9 M)	HPC	EC	DBS
F <sub>1</sub>	30	30	—	40	—	—
F <sub>2</sub>	30	—	30	40	—	—
F <sub>3</sub>	30	30	—	—	40	5.2
F <sub>4</sub>	30	—	30	—	40	5.2

Abbreviations: PEO: Polyethylene oxide; HPC: Hydroxypropyl cellulose; EC: Ethyl cellulose; DBS: Dibutyl sebacate.

mm were selected for printing tablets. The computer-aided design (CAD) model of a cylindrical tablet was designed online using Tinker CAD and then exported as an STL file, which was imported to the software Makerbot Replicator 2X printer (Makerbot Inc., USA). Printed tablets had a height of 4.5 mm and a diameter of 9.5 mm. Based on the preliminary experiments, those dimensions were selected (i) to get the same tablet weights as those prepared by other methods (333.3 mg) and (ii) to get a similar surface area (SA)/volume (V) ratio as other tablets ( $0.8 \text{ mm}^{-1}$ ). This enables a more accurate comparison, as weight and SA/V can have an impact on drug release profiles. Printing settings were as follows: layer height: 0.2 mm; infill density: 100%; number of shells: 2; printing speed: 90 mm/s; bed temperature: 50°; and nozzle temperature: 220°.

#### 2.4. Differential scanning calorimetry

The solid-state and thermal behavior of raw materials and formulations was investigated using differential scanning calorimetry (DSC) 4000 system (Perkin Elmer, USA). It was used to determine the  $T_m$  and  $T_g$  of EC and HPC, as well as the  $T_m$  of PEO, theophylline, and each of the formulations. Approximately 6 mg of each material or formulation was placed into crucible aluminum pans, and samples were scanned from 25 to 300°, encompassing the high temperatures used in HME and printing methods. The samples were scanned at a scanning rate of 10°/min with nitrogen purging at a flow rate of 20 mL/min. The obtained DSC traces were analyzed using Pyris software (Perkin Elmer, USA).

#### 2.5. X-ray powder diffraction

To investigate the effect of extrusion and 3D printing on the crystallinity of the formulations, X-ray powder diffraction (XRPD) patterns of theophylline, PEO, EC, HPC, PM tablets, HME tablets, and FDM tablets were determined using a Siemens D500 X-ray diffractometer (Siemens, Germany) with copper radiofrequency (Rf) radiation at 40 kV voltage and 30 mA. Data were recorded at  $2\theta$  of 5–50° at a step width of 0.01° and 1 s time count. XRPD samples are preferably in powder form, which was possible for PM and HME samples. However, 3D-printed tablets were too hard to grind; thus, thin films were printed, followed by manual grinding using a pestle and mortar to achieve finer samples. Peak intensity is an arbitrary factor in this study since tested samples were varied in their weight and particle size; thus, diffractograms were compared for any changes in peak shape, position, and broadening to assess crystallinity.

#### 2.6. Gel permeation chromatography

Gel permeation chromatography (GPC) was run in a 1260 Infinity GPC system (Agilent, UK) equipped

with a refractive index detector. Samples for GPC were prepared in 1 mg/mL solutions by dissolving formulation powders in dimethyl formamide (DMF) containing 5 mM  $\text{NH}_4\text{BF}_4$  and 0.25/100 mL of toluene at 40° for 30 min. In-house experiments revealed that samples were not dissolved by stirring over 24 h at room temperature ( $25 \pm 2^\circ$ ). Thus, heating was essential to achieve complete solubility when preparing the samples. Thereafter, 100  $\mu\text{L}$  of the sample was injected into a PLgel 5  $\mu\text{m}$  guard column ( $50 \times 7.5 \text{ mm}$ ), followed by two PLgel 5  $\mu\text{m}$  MIXED-D ( $300 \times 7.5 \text{ mm}$ ) columns at 60°. The mobile phase was DMF containing 5 mM  $\text{NH}_4\text{BF}_4$  at a flow rate of 1 mL/min. Despite the protocol being developed in-house, it is relatively similar to other protocols where DMF and gentle heating were used with PEO samples.<sup>18,19</sup>

As the aim was to find the impact of different processing conditions on PEO  $M_w$ , a comparative study was conducted without using a reference standard. In brief, GPC experiments were conducted with PEO in its pure form and in formulations processed via three distinct methods (PM, HME at 150°, and FDM at 220°). After the GPC test, all obtained chromatographs were compared against each other (a comparative study).

#### 2.7. Particle size analysis of ground filaments

Particle size distribution was measured manually using a nest of five small sieves with different aperture sizes (63, 150, 250, 600, and 2000  $\mu\text{m}$ ). Sieving time was 3 min, where sieves were agitated in linear and circular motions with repeated tapping. The sample weight was around 2 g. The starting weight of the sample was recorded and the weight of powder retained on each sieve after the sieving test was also recorded and converted to % of mass retained on each sieve (frequency%). Size distribution was plotted based on the retained mass % against the aperture size of the sieve. The average size (A) was calculated based on the retained mass % ( $w_i$ ) in each sieve and sieve diameter ( $d_i$ ), as presented in Equation I:<sup>20</sup>

$$A = \frac{\sum w_i \times d_i}{\sum w_i} \quad (1)$$

#### 2.8. Tablet characteristics

Tablets were characterized in terms of their weight, SA/V ratio, hardness, and porosity. True density was also measured using a helium pycnometer (AccuPyc II 1340; Micromeritics, USA) since the thermal process can alter the true density of the material, as reported in previous work.<sup>16</sup> The density of physical mixture powders, ground filaments, and ground printlets were considered the true



density for PM, HME, and printed tablets, respectively. The hardness of tablets was estimated using a hardness tester (TBH 125 series; Erwaka, Germany). Surface area and volume were calculated based on the dimensions of tablets measured using a vernier caliper. To calculate the approximate porosity of the obtained tablets, the average apparent density of tablets ( $n = 3$ ) was calculated from their volume and weight. The porosity of all tablets was then calculated by employing **Equation II**:

$$P\% = 1 - \frac{D_a}{D_t} \times 100 \quad (\text{II})$$

where  $P$  is the porosity,  $D_a$  is the apparent density, and  $D_t$  is the true density.

### 2.9. *In vitro* dissolution studies and calculations

Dissolution tests were carried out for tablets ( $n = 3$ ) under sink conditions using a USP type II paddle apparatus (708-DS Dissolution Apparatus; Agilent Technologies, USA) attached to a UV spectrophotometer (Cary 60 UV-Vis; Agilent Technologies, USA). The vessels were filled with 900 mL of deionized water (based on USP); the temperature was set at  $37 \pm 1^\circ$ ; and the paddle rotation speed was set at 50 rpm. The test duration was 12 h with readings, i.e., the absorbance was measured every 10 min for the first two hours, then every 30 min thereafter. The wavelength used to measure the absorbance of theophylline was 271 nm.<sup>21</sup> Drug release profiles were plotted as the percentage of cumulative drug release versus time (h).

The dissolution data was analyzed using several different measures. First, a quantitative comparison of the dissolution behavior of different tablets was performed using dissolution efficiency (DE%). Next, a qualitative comparison was conducted using similarity ( $f_2$ ) and difference ( $f_1$ ) factors to support the quantitative comparison. Here, similar dissolution profiles have a similarity factor ( $f_2$ ) of  $\geq 50$ .<sup>22</sup> Finally, the drug release kinetics were analyzed using DDSolver software (an add-in program in Microsoft Excel).<sup>23</sup> In this analysis, several drug release kinetic models were examined to find the best fit, including the zero-order, first-order, Higuchi, and Korsmeyer-Peppas models. As a measure of statistical fit,  $R^2_{\text{adj}}$  was used, where higher  $R^2_{\text{adj}}$  values indicate a better fitting model. In the Korsmeyer-Peppas model, the  $n$  value can indicate the drug release mechanism if up to 60% of the drug has been released.<sup>24</sup> When  $n < 0.45$ , the drug release is governed by diffusion (Fickian model); when  $n > 0.89$ , swelling is the main release mechanism and close to zero-order kinetics (non-Fickian model). When  $0.45 <$

$n < 0.89$ , drug release is governed by both diffusion and swelling mechanisms.<sup>24–26</sup>

### 2.10. Statistical analysis

For dissolution data, as discussed in **Section 2.9**,  $f_2$  and  $f_1$  factors were used as model-independent statistical approaches to compare the dissolution profiles of different tablets,<sup>22</sup> along with parameters from kinetics analysis and DE%. For other experimental data, the significance of differences in porosity, hardness, and density of formulations was analyzed using analysis of variance (ANOVA). The significance level (alpha) was set at 0.05. Two-way ANOVA was used, as the impact of the manufacturing method was studied across different formulations (two independent variables, manufacturing methods, and formulations).

## 3. Results and discussion

### 3.1. Selection of polymers and manufacturing methods

High  $M_w$  PEOs ( $\geq 0.9$  M) have the potential to prolong drug release, making it a viable option in formulation design of controlled release formulations. However, their high melt viscosity and  $M_w$  instability restrict their application in FDM 3D printing. As a result, formulation scientists who are interested in using PEO in 3D printing formulations would likely mix this polymer with other ingredients to improve printability, since PEO is too viscous to be printed alone. Here, formulations were developed to include PEO mixed with thermally stable and low-viscosity polymers, HPC or EC, with theophylline as the model drug. The developed formulations ( $F_1$ – $F_4$ ) were made into tablets via three methods with varying thermal and mechanical processing conditions. The methods were direct compression of PMs, direct compression of HMEs, and FDM 3D printing. The resulting tablets of each formulation ( $F_1$ – $F_4$ ) underwent different physical tests to identify changes in thermal behavior, PEO  $M_w$ , crystallinity, and theophylline release profile.

### 3.2. Differential scanning calorimetry

Differential scanning calorimetry (DSC) was performed at  $25$ – $300^\circ$ , encompassing the high temperatures used in HME ( $140^\circ$ ) and the printing process ( $220^\circ$ ). DSC graphs of the processed formulations were compared with those of the starting materials to investigate any changes in their thermal behavior due to the processing conditions (**Figures 1** and **2**). Since all formulations displayed similar patterns, only the DSC traces of formulation  $F_2$  are presented to avoid repetition.

Ethyl cellulose (EC) is an amorphous polymer that exhibits a flat thermogram, and adding DBS to EC can

induce a plasticizing effect on the EC polymer. HPC is also an amorphous polymer that exhibits a flat line. Its glass transition temperature should be between 100–120°,<sup>27</sup> but this was hardly detectable in the DSC graph as mentioned in other studies.<sup>28</sup> For PEO, the two  $M_w$  (0.9 and 7 M) displayed relatively similar melting points at 73.74 and 73.06°, respectively. In agreement with this, it has been reported that high  $M_w$  PEOs typically have relatively similar  $T_m$  values.<sup>9,11</sup> The  $T_g$  value of PEO (−50°<sup>29</sup>) was not the focus of this study. The melting point of the original theophylline was found to be approximately 273°.

The DSC traces of the various processed formulations exhibited the signature PEO and theophylline melting peaks, indicating the presence of their crystalline forms. The  $T_g$  of EC in  $F_3$  and  $F_4$  tablets was hardly detectable, which could be attributed to the positioning of the EC  $T_g$  immediately after the PEO melting peak. This could have caused the peaks to merge, making it difficult to observe a separate  $T_g$  peak. The  $T_m$  of theophylline decreased from approximately 273° in its pure form to 243–250° in PM, HME, and 3D-printed samples for all formulations, which

can be attributed to its intermolecular interaction with polymers used in the formulations.

The  $T_m$  of PEO in PM samples was ~72°, which decreased to ~66° for HME and ~64° for printed samples. This pattern was also noticed in another study where  $T_m$  of PEO decreased for HME.<sup>13</sup> Table 2 displays changes in the  $T_m$  of PEO in each formulation. The decrease in  $T_m$  could result from PEO depolymerization (i.e., reduction of  $M_w$  following degradation) or a reduction in its crystallinity. PEO undergoes crystallinity reduction after a thermal process, further reducing its  $T_m$  by 7°.<sup>2,30</sup> Additionally, it has been suggested that mixing PEO with amorphous polymers can restrict its recrystallization after cooling, leading to a drop in  $T_m$  following thermal processing.<sup>31</sup> To examine these mechanisms, GPC was employed, which reported a reduction in  $M_w$  of PEO in HME and 3D-printed samples that may contribute to the reduction in  $T_m$  (discussed in Section 3.4).

### 3.3. X-ray powder diffraction

X-ray powder diffraction (XRPD) was employed at  $2\theta$  at 5–50° for raw materials and processed samples

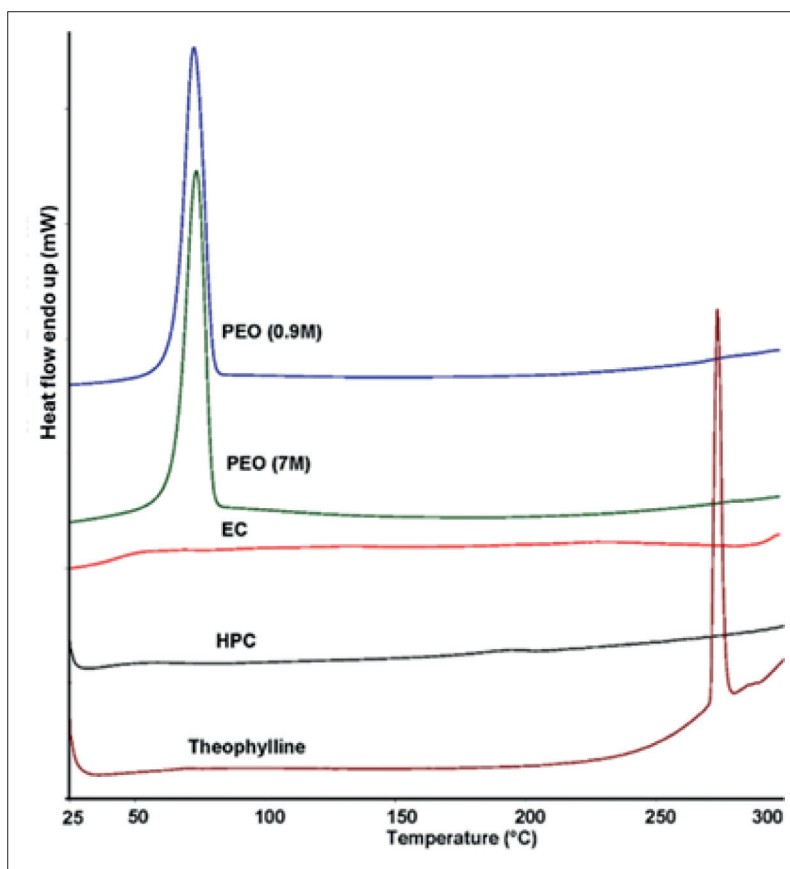


**Figure 1.** Differential scanning calorimetry (DSC) curves of the starting materials used in this study. Abbreviations: PEO: Polyethylene oxide; HPC: Hydroxypropyl cellulose; EC: Ethyl cellulose.

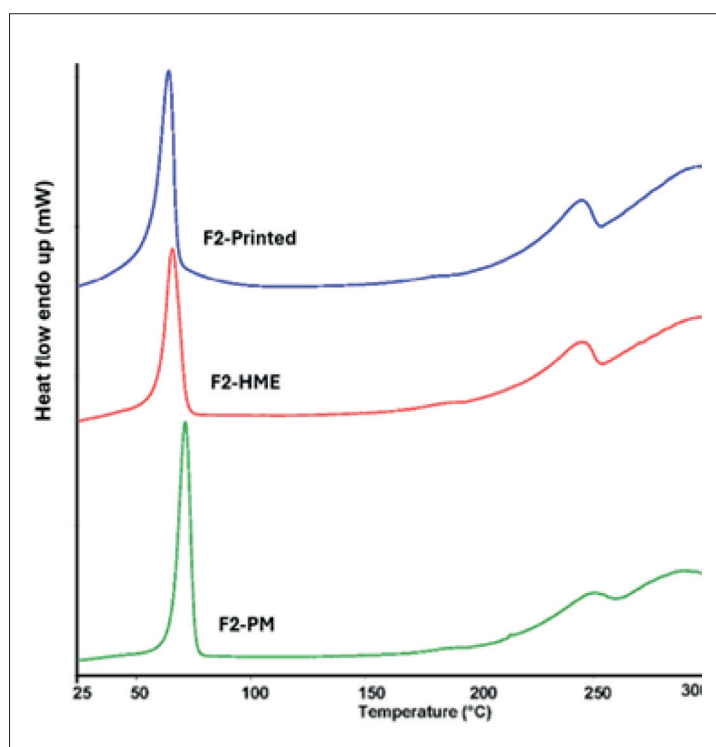


**Figure 2.** Differential scanning calorimetry (DSC) traces of physical mixture (PM), hot-melt extrudate (HME), and printed samples of formulation F<sub>2</sub>. Since all formulations displayed similar patterns, only DSC traces of F<sub>2</sub> are presented to avoid repetition.

**Table 2.** Melting point ( $T_m$ ) of polyethylene oxide (PEO) after each process.

Formulation	$T_m$ , mean $\pm$ SD (°)		
	PM	HME	Printed
F <sub>1</sub>	72.11 $\pm$ 0.15	67.06 $\pm$ 0.82	64.42 $\pm$ 0.32
F <sub>2</sub>	71.18 $\pm$ 0.37	65.61 $\pm$ 0.51	65.13 $\pm$ 1.22
F <sub>3</sub>	71.87 $\pm$ 0.25	67.06 $\pm$ 1.51	65.41 $\pm$ 1.33
F <sub>4</sub>	71.24 $\pm$ 0.28	66.3 $\pm$ 1.43	64.86 $\pm$ 2.30

Note: SD is calculated from the mean of triplicates. Abbreviations: PM: Physical mixture; HME: Hot-melt extrudates.

(Figures 3 and 4). Theophylline is a crystalline material whose diffractogram displays numerous sharp peaks, with the highest peak at a  $2\theta$  of  $12.6^\circ$ . EC and HPC exhibited a halo-shape diffractogram due to their amorphous structures. The diffractogram of PEO, a semi-crystalline polymer, exhibited characteristic crystalline peaks at  $2\theta$  of  $18.8^\circ$  and  $23^\circ$ . Since both  $M_w$  of PEO have similar characteristics according to previous studies<sup>11</sup> and proved similar in DSC tests, only PEO 7 M was studied for crystallinity in this work.

Meanwhile, in the diffractograms of formulations, the characteristic peaks of theophylline and PEO were detected, indicating the presence of both materials in the crystalline state. However, some noticeable changes can

be observed in the peak position, shape, and width in thermally processed samples compared to non-thermally processed samples. Since all formulations displayed similar diffractograms, only the diffractogram for F<sub>2</sub> is presented (Figure 4) to avoid repetition.

Changes in crystal structure and lattice strain can result in peak split,<sup>32</sup> a phenomenon noticed in PEO peaks, especially in formulations F<sub>3</sub> and F<sub>1</sub> containing PEO 7 M (Figure 4). Moreover, there was a broadening in all crystalline peaks of HME and printed samples compared to PM samples, reflecting a change in crystal size or lattice also reported in other studies.<sup>3,6</sup> Overall, based on peak broadening and deformation, as well as the findings of other studies, PEO appears to have exhibited a change in

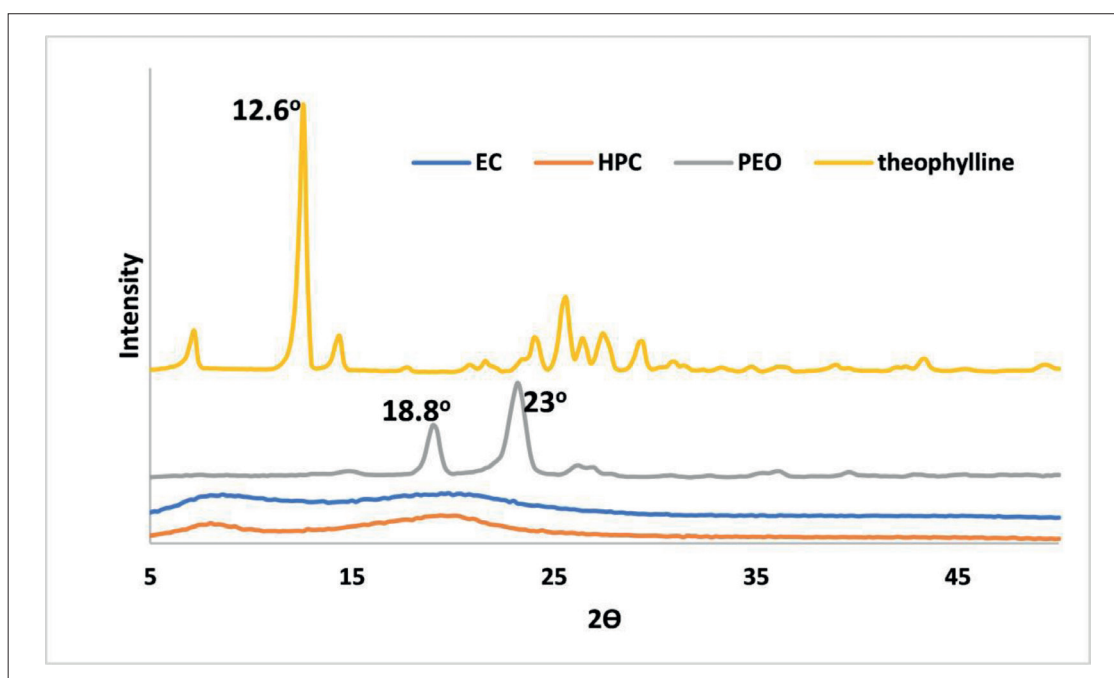


**Figure 3.** X-ray powder diffraction (XRPD) diffractograms of raw materials. Abbreviations: PEO: Polyethylene oxide; HPC: Hydroxypropyl cellulose; EC: Ethyl cellulose.

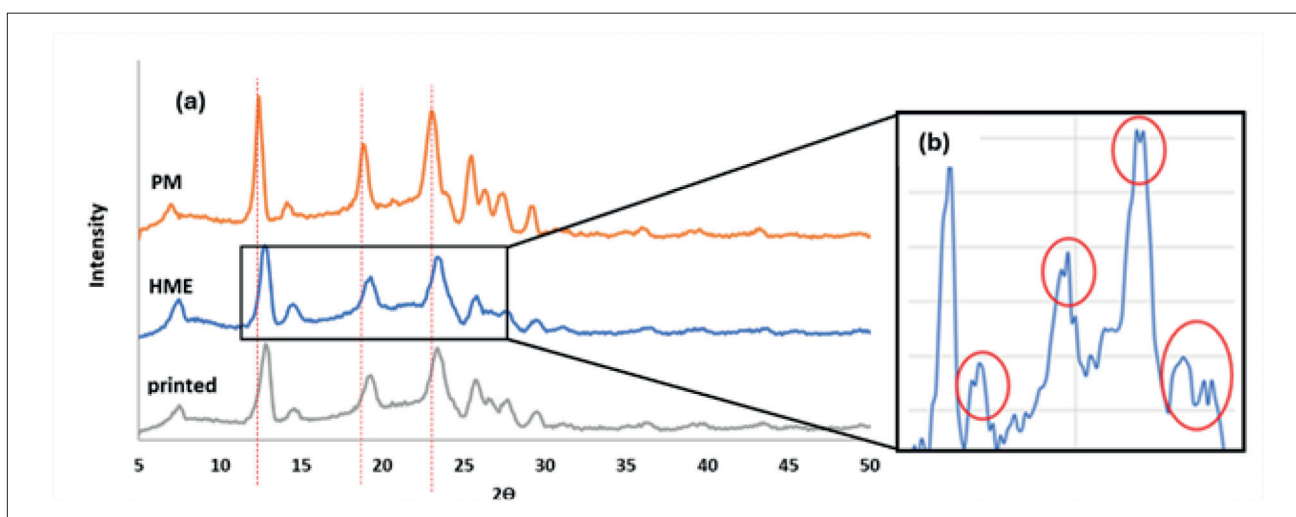


**Figure 4.** Changes of crystal form after thermal process (a) X-ray powder diffraction (XRPD) diffractograms of physical mixture (PM), hot-melt extrudate (HME), and printed samples of formulation  $F_2$ . (b) The 10–30° region of  $2\theta$  displays peak splits in thermally processed samples.

crystal size, crystalline lattice, strain, and crystallinity (%) upon heating.<sup>3,6</sup> Such changes can modify the drug release rate, as mentioned in another work.<sup>7</sup>

### 3.4. Gel permeation chromatography

Gel permeation chromatography (GPC) analysis was performed with pure PEO (7 M) samples and various processed  $F_1$  formulations (PM, HME, and FDM) (Figure 5). The aim was to identify any changes in the

$M_w$  of PEO following thermal and mechanical stress due to processing conditions. Given that all formulations displayed a massive surge in release rate after the first thermal process (i.e., HME), we focused only on one formulation (i.e.,  $F_1$ ) for subsequent GPC studies to evaluate  $M_w$  changes in PEO.

Pure PEO 7 M exhibited a single peak with a retention time of 9.44 min in the chromatogram (black line in Figure 5a).



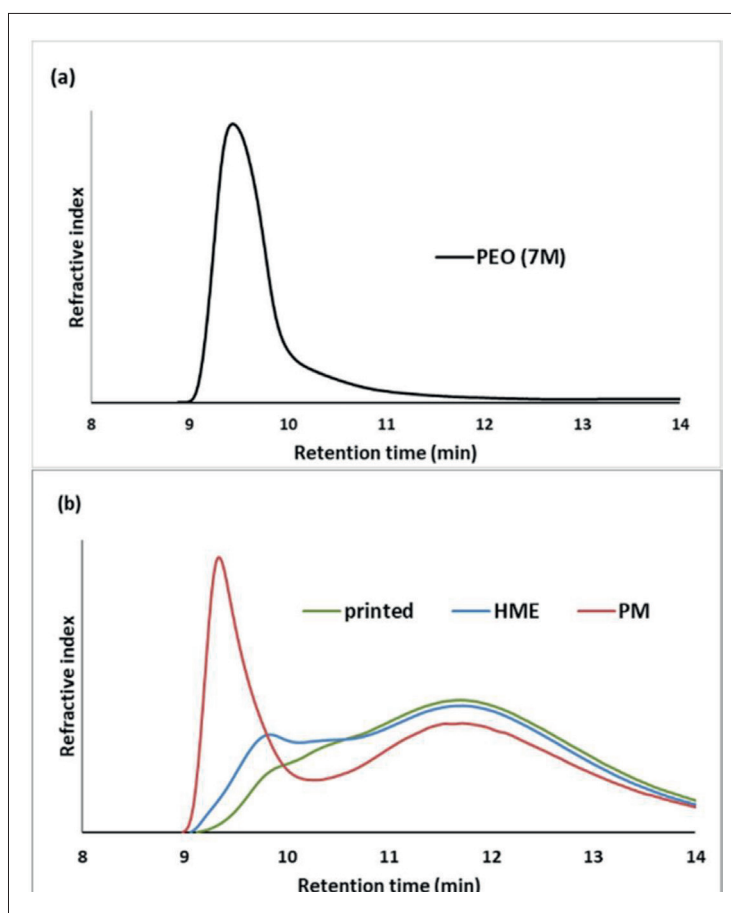


**Figure 5.** Gel permeation chromatography (GPC) chromatograms of (a) pure polyethylene oxide (PEO; 7M) and (b) physical mixture (PM), hot-melt extrudate (HME), and printed samples of  $F_1$ , displaying reduction and shifts in peak 1 due to PEO degradation after each thermal process.

PM samples (red line in Figure 5b) exhibited two signals; a sharp peak (peak 1) at the same retention time of PEO 7 M (~9.5 min) and a broader peak (peak 2) at 10–14 min, indicating HPC in the PM formulation. However, the intensity of the PEO 7 M signal at peak 1 in HME and printed samples decreased significantly compared to PM samples despite having the same starting composition and concentration. The relative intensity of each peak was calculated and reported in Table 3.

Chromatograms for HME and 3D-printed tablets (Figure 5) display a delayed peak 1 signal with obvious

**Table 3. Relative intensity of peaks 1 and 2 after each manufacturing process.**

Sample	Relative intensity of peak 1/peak 2
PM	1.47
HME	0.9
Printed	0.45

Abbreviations: PM: Physical mixture; HME: Hot-melt extrudates.

broadening. Moreover, the ratio of the intensity of the peaks (PEO to HPC; peak 1/peak 2) decreased in the order: PM > HME > 3D-printed samples. These observations can be explained by the reduction in PEO  $M_w$  during processing, resulting in smaller chains with higher retention time. The 3D-printed samples undergo two thermal processes: one in HME while making filament extrudates and another in the 3D printer; thus, these samples exhibit the highest reduction in the PEO 7 M signal (peak 1).

### 3.5. Particle size analysis of ground filaments

Grinding the HME filaments of all the developed formulations in this study resulted in coarse, flake-shaped particles (Figure 6), whereas the PM powders were fine (<400  $\mu\text{m}$ ). The size distribution and arithmetic average particle size were determined using sieves.<sup>20</sup> Figure 7 displays the particle size distribution of ground filaments of all formulations. The plasticity of PEO results in coarse particles with irregular shapes upon grinding the filaments. For thermoplastic polymers, like PEO, it is challenging to obtain fine particles due to plastic deformation rather than

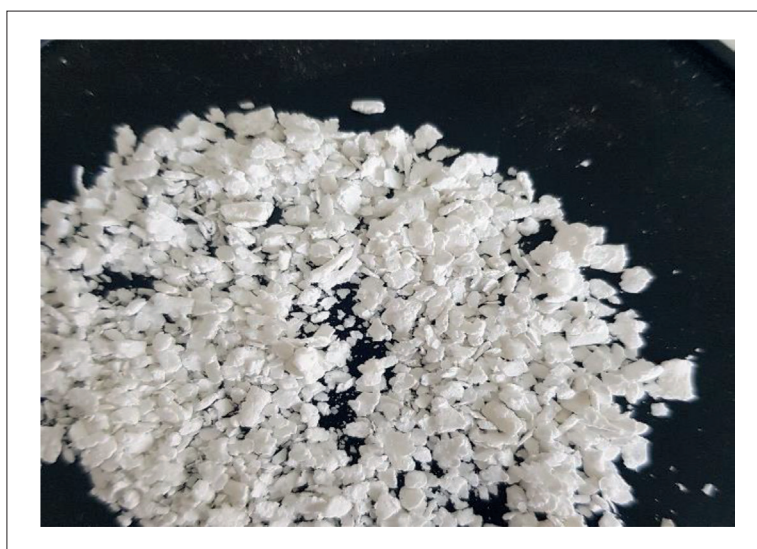


Figure 6. Flak-shaped powders after grinding filaments in the ball mill.

brittle fracture under conventional grinding methods,<sup>33,34</sup> such as ball-milling used in this study. Usually, cryogenic or wet grinding is employed to produce fine particles of plastic polymers.<sup>33,34</sup>

Regardless of the  $M_w$  of PEO, it is obvious that grinding the filaments containing EC ( $F_3$  and  $F_4$ ) produces considerably larger particles compared to those containing HPC ( $F_1$  and  $F_2$ ). The arithmetic average sizes of  $F_3$  and  $F_4$  ground filaments were 1352.69 and 1796.91  $\mu\text{m}$ , respectively, while those for  $F_1$  and  $F_2$  were much smaller at 530.56 and 919.47  $\mu\text{m}$ , respectively. The large particle

size of EC-containing formulations can be attributed to the presence of DBS plasticizer in EC fractions. The addition of plasticizers can increase material ductility and reduce its brittleness, increasing the average particle size of the ground material.<sup>35</sup>

Regarding the  $M_w$  of PEO, formulations with PEO of a higher  $M_w$  (e.g., 7 M) produced finer particle sizes upon grinding the filaments. Ground filaments of  $F_1$  containing HPC/PEO 7 M had a smaller average size than that of  $F_2$  containing HPC/PEO 0.9 M (530.56 vs. 919.47  $\mu\text{m}$ , respectively). Similarly, the average size of  $F_3$

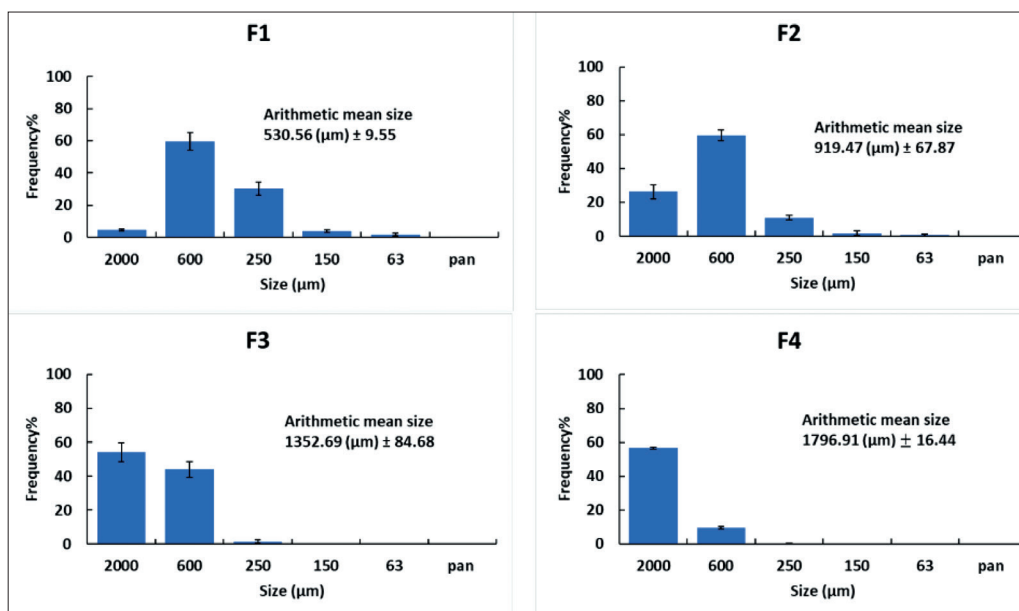


Figure 7. Size distribution based on the retained fraction (%) in each sieve for ground filaments of all formulations, presented as the mean  $\pm$  SD for each formula. Abbreviation: pan: powder size <63  $\mu\text{m}$ .

**Table 4. Hardness of prepared tablets.**

Formulation	Hardness, mean $\pm$ SD (N)		
	Printed	HME	PM
F <sub>1</sub>	>300	216 $\pm$ 13	239 $\pm$ 6
F <sub>2</sub>	>300	242 $\pm$ 19	236 $\pm$ 25
F <sub>3</sub>	203 $\pm$ 10	170 $\pm$ 14	202 $\pm$ 7
F <sub>4</sub>	256 $\pm$ 23	154 $\pm$ 7	211 $\pm$ 2

Note: SD is calculated from the mean of triplicates. Abbreviations: PM: Physical mixture; HME: Hot-melt extrudate.

ground filaments containing EC/PEO 7 M was smaller than F<sub>4</sub> containing EC/PEO 0.9 M (1352.69 vs. 1796.91  $\mu$ m, respectively). Generally, high  $M_w$  PEO resins have relatively similar mechanical characteristics.<sup>11</sup> However, the inclusion of other materials can restrict the PEO polymer chain mobility and increase internal stress among formulations, resulting in stiffer formulations when compared to the use of lower  $M_w$  PEOs.<sup>36</sup> Having a brittle material can usually result in finer particle size.<sup>33</sup> Thus, the observed particle size reduction in ground F<sub>1</sub> vs. F<sub>2</sub> and ground F<sub>3</sub> vs. F<sub>4</sub> could be attributed to changes in PEO  $M_w$ .

### 3.6. Characterization of tablets

To rule out the effect of tablet weight and SA/V on the drug release profile, tablets from different processing methods were designed to have the same average weight (333.3 mg) and SA/V (0.8 mm<sup>-1</sup>). The hardness, true density, apparent density, and porosity were measured for all the tablets (Tables 4–7). The results indicate that tablet hardness decreased in the order of 3D-printed > PM  $\geq$  HME samples for most formulations. The 3D-printed tablets were the hardest (Table 4), probably due to the nature of the printing method, where tablets made of molten layers could produce stronger consolidation.<sup>16</sup> HME tablets appeared to be less hard than PM and printed tablets. For example, HME tablets of F<sub>4</sub> had a hardness of 154 N compared to 211 and 256 N for PM and printed tablets, respectively. These hardness results can be attributed to differences in particle size between PM powders and HME

ground filaments. As previously discussed, HME ground filaments were much larger than PM.<sup>37,38</sup> Furthermore, PEO degradation, reported in GPC data, can reduce the mechanical strength of HME samples and the resulting tablets' hardness.

Notably, the formulation composition can impact the hardness of tablets. Tablets prepared from formulations containing PEO/HPC mixture (F<sub>1</sub> and F<sub>2</sub>) are considerably harder than those prepared from EC/PEO (F<sub>3</sub> and F<sub>4</sub>). For example, 3D-printed tablets of F<sub>1</sub> and F<sub>2</sub> had a hardness of over 300 N (beyond the detection limit of the hardness tester), while those of F<sub>3</sub> and F<sub>4</sub> had a hardness of 203–256 N. This can be due to the presence of DBS in F<sub>3</sub> and F<sub>4</sub>, as the plasticizer can improve the flexibility of the polymer, making it less resistant to deformation.<sup>35</sup>

Since thermal processes can alter the specific volume of polymers,<sup>39,40</sup> the true density of the processed formulations will be affected. The results reported in Table 5 indicate a decrease in true density after 3D printing, which was significant for F<sub>1</sub> and F<sub>2</sub> but not for F<sub>3</sub> and F<sub>4</sub>. Rapid heating/cooling occurs during 3D printing, where the materials' temperature fluctuates between room temperature and 220° within 4–5 min, affecting the formulations' true density.

Apparent density (Table 6) also featured a noticeable reduction after thermal processing, indicating the significant impact of the manufacturing method on density ( $p < 0.05$ ). The apparent density of printed tablets was  $\sim 1$  g/cm<sup>3</sup>,

**Table 5. True density of tablets for various formulations obtained via different manufacturing methods.**

Formulation	True density, mean $\pm$ SD (g/cm <sup>3</sup> )		
	Printed	HME	PM
F <sub>1</sub>	1.215 $\pm$ 0.001	1.293 $\pm$ 0.001	1.282 $\pm$ 0.002
F <sub>2</sub>	1.198 $\pm$ 0.001	1.294 $\pm$ 0.002	1.28 $\pm$ 0.002
F <sub>3</sub>	1.245 $\pm$ 0.002	1.261 $\pm$ 0.003	1.264 $\pm$ 0.002
F <sub>4</sub>	1.25 $\pm$ 0.002	1.27 $\pm$ 0.002	1.26 $\pm$ 0.002

Note: SD is calculated from the mean of triplicates. Abbreviations: PM: Physical mixture; HME: Hot-melt extrudate.

**Table 6. Apparent density of tablets for various formulations obtained via different manufacturing methods.**

Formulation	Apparent density, mean $\pm$ SD (g/cm <sup>3</sup> )		
	Printed	HME	PM
F <sub>1</sub>	0.995 $\pm$ 0.015	1.184 $\pm$ 0.011	1.184 $\pm$ 0.011
F <sub>2</sub>	1.001 $\pm$ 0.022	1.173 $\pm$ 0.017	1.166 $\pm$ 0.010
F <sub>3</sub>	0.998 $\pm$ 0.020	1.147 $\pm$ 0.012	1.137 $\pm$ 0.011
F <sub>4</sub>	1.017 $\pm$ 0.029	1.145 $\pm$ 0.019	1.133 $\pm$ 0.017

Note: SD is calculated from the mean of triplicates. Abbreviations: PM: Physical mixture; HME: Hot-melt extrudate.

much lower than that for PM and HME tablets ( $\sim$ 1.18 g/cm<sup>3</sup>), indicating the high porosity of the printed tablets.

Porosity was calculated using the values of true and apparent densities, decreasing in the order: 3D-printed > HME  $\sim$  PM (Table 7). Since printed tablets of all formulations have significantly lower true and apparent densities, they are expected to be the most significantly porous compared to HME and PM ( $p < 0.05$ ). This trend was also noticed in our previous work for 3D-printed tablets due to the layer-by-layer printing, forming gaps between the tablet layers.<sup>16</sup> Conversely, despite their high porosity, the printed tablets did not exhibit the lowest hardness compared to the other samples in this study, suggesting that the solidification of molten layers in 3D printing leads to stronger consolidation of tablet compartments, as previously observed.<sup>16</sup> Both HME and PM tablets have relatively similar porosities ( $p > 0.05$ ), despite their significant differences in hardness. Therefore, hardness differences between HME and PM tablets are likely due to the impact of their particle size, manufacturing method, and formulation composition rather than the porosity.

### 3.7. *In vitro* dissolution studies

Dissolution profiles of tablets manufactured from the four formulations are displayed in Figures 8 and 9. DE% and similarity factors were calculated to compare the dissolution data. To elaborate on the dissolution profiles, tablets hardness, porosity, formulation composition, and  $M_w$  changes after thermal stress were considered. The

effect of particle size on dissolution rate is not comparable between different manufacturing methods; in PM tablets, the particles of each material were mixed physically, whereas, in HME and 3D-printed tablets, the particles were mixed molecularly as a result of melting. Hence, the nature of particles is relatively different from each other. Moreover, in 3D-printed tablets, there were no particle sizes to be studied as they were made of molten layers.

Comparing the dissolution profiles displayed a considerable increase in DE% for all formulations as a result of the HME process (Figures 8 and 9). For example, the DE% of F<sub>1</sub> and F<sub>2</sub> increased from 26.48 and 49.58% for PM tablets to 75.05 and 73.79% for HME tablets, respectively. F<sub>3</sub> and F<sub>4</sub> also demonstrated similar patterns. These results corroborate the GPC findings, indicating a reduction in PEO  $M_w$  in HME samples, which can result in faster drug release. Moreover, HME tablets were less hard than PM tablets (Table 4), which can also be responsible for the faster theophylline release. Furthermore, the reduction in crystal size after HME, as observed from XRPD, can play a role in increasing DE%.<sup>7</sup> The  $f_2$  between HME and PM tablets was in the range of 17.36–44.57%, which is an indication of a significant difference between the dissolution profiles of PM and HME tablets.

The GPC data displayed a further reduction in PEO  $M_w$  in printed tablets, and along with the increased porosity of these tablets should have increased the DE% for the 3D-printed tablets compared to HME tablets. However,

**Table 7. Porosity of tablets for various formulations obtained via different manufacturing methods.**

Formulation	Porosity, mean $\pm$ SD (%)		
	Printed	HME	PM
F <sub>1</sub>	17.85 $\pm$ 1.195	8.399 $\pm$ 0.467	8.218 $\pm$ 0.841
F <sub>2</sub>	16.685 $\pm$ 2.624	9.357 $\pm$ 1.296	8.919 $\pm$ 0.801
F <sub>3</sub>	19.80 $\pm$ 1.627	9.045 $\pm$ 0.938	10.015 $\pm$ 0.908
F <sub>4</sub>	18.492 $\pm$ 2.287	9.804 $\pm$ 1.476	10.083 $\pm$ 1.318

Note: SD is calculated from the mean of triplicates. Abbreviations: PM: Physical mixture; HME: Hot-melt extrudate.



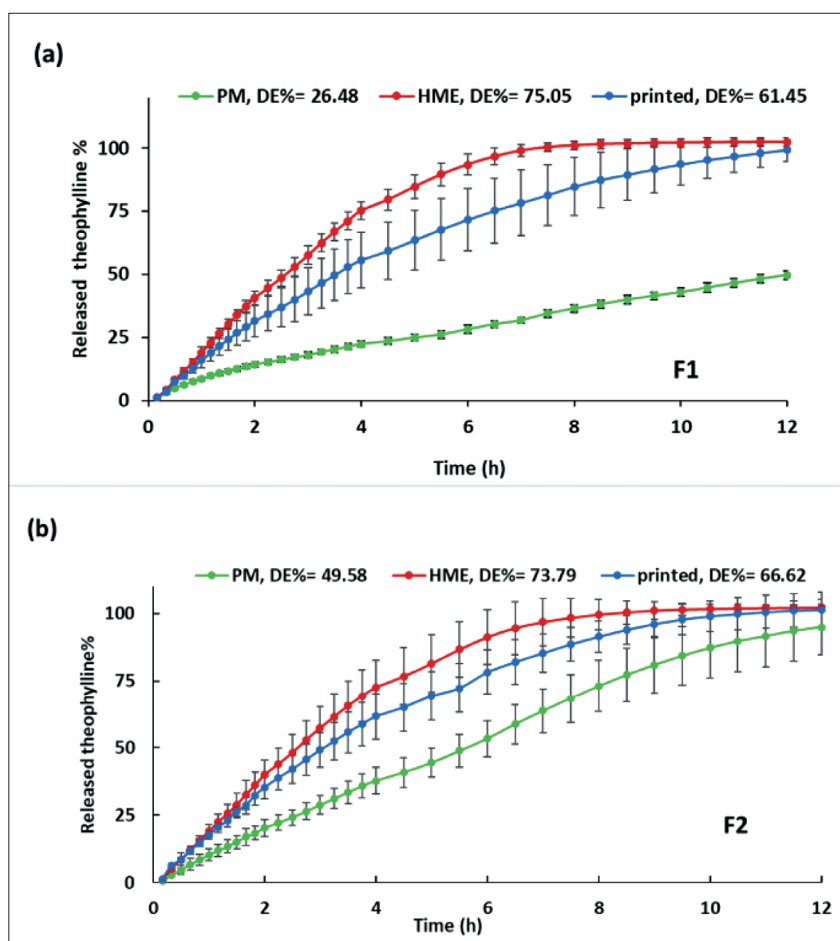


**Figure 8.** Dissolution curves of  $F_1$  (a) and  $F_2$  (b), presented with error bars and the dissolution efficiency (DE%) values for the physical mixture (PM), hot-melt extrudate (HME), and 3D-printed tablets.

this was not the case, and the DE% of printed tablets was less than that of HME tablets. For example, in  $F_1$  and  $F_3$ , DE% decreased from 75.05 and 53.4% in HME tablets to 61.45 and 24.1% in 3D-printed tablets, respectively. Therefore, drug release from these tablets appeared to be more impacted by their significantly increased hardness rather than  $M_w$  reduction and porosity changes. Moreover, 3D-printed and HME tablets have dissimilar release behavior ( $f_2 < 50$ ) in all tablet formulations except for  $F_2$  ( $f_2 = 56.53\%$ ). The  $f_2$  values for dissolution profiles of HME compared to 3D-printed tablets of  $F_1$ – $F_4$  were 43.89, 56.53, 27.97, and 30.05%, respectively.

The printing method also improved the tablet's integrity when used for formulations containing EC, as printed tablets of  $F_3$  and  $F_4$  remained intact during the dissolution and did not disintegrate. In contrast, HME tablets were completely disintegrated during the dissolution test. The lack of disintegration of 3D-printed tablets results in low contact surface area with the dissolution medium, thus

further delaying the dissolution process. For example, DE% of  $F_3$  was 24.1% in printed tablets compared to 53.4% in HME tablets. This supports our previous findings and suggests that 3D printing can extend drug release when hydrophobic polymers, like EC, are incorporated into the formulation.<sup>16,26</sup> Notably, maintaining the integrity of 3D-printed tablets of  $F_3$  and  $F_4$  could prolong drug release compared to the tablets obtained via the PM method, despite the noticeable reduction in PEO  $M_w$  after printing. DE% of  $F_3$  and  $F_4$  was 24.1 and 25.77% for printed tablets compared to 28.05 and 38.7% for PM tablets, respectively.

Besides the manufacturing method, the type of materials used in formulations can also modulate drug release from tablets. For polymer mixtures, the dissolution behavior is determined by each polymer's contribution to the formulation, as well as the interaction of all the components with each other and the drug. This interplay between components is expected to be influenced by the tablet manufacturing method.<sup>16</sup>

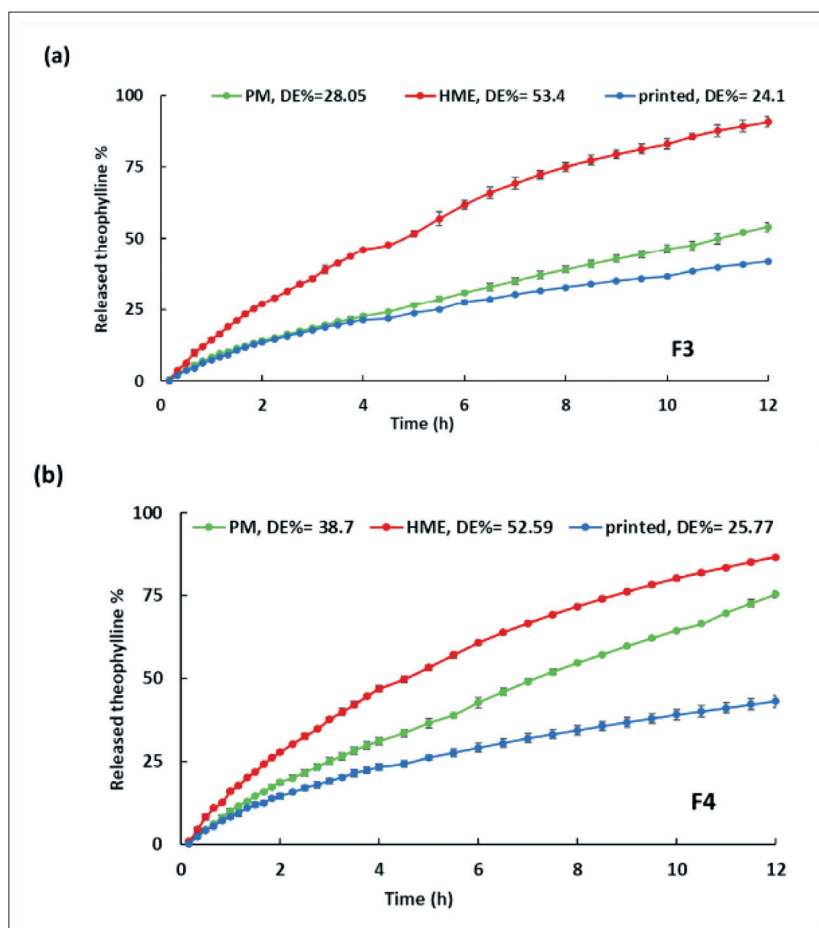


**Figure 9.** Dissolution curves of F<sub>3</sub> (a) and F<sub>4</sub> (b), presented with error bars and the dissolution efficiency (DE%) values for physical mixture (PM), hot-melt extrudate (HME), and 3D-printed tablets.

Figure 10 displays the dissolution profiles of the four formulations (F<sub>1</sub>–F<sub>4</sub>) made into PM tablets. The smaller standard deviation bars observed indicate that the dissolution behavior is more consistent in F<sub>3</sub> and F<sub>4</sub> tablets containing EC (as opposed to HPC in F<sub>1</sub> and F<sub>2</sub>). An overall faster release for F<sub>2</sub> and F<sub>4</sub> containing 0.9 M PEO infers the impact of the  $M_w$  of PEO; formulations containing the 7 M PEO (F<sub>1</sub> and F<sub>3</sub>) have a stronger gelling behavior and slower release. The strong gelling behavior of PEO 7 M appears to dominate the effects of HPC in F<sub>1</sub> and EC in F<sub>3</sub>, as both formulations have similar dissolution profiles ( $f_2 = 84.86$ ). However, the effect of HPC (hydrophilic) or EC (hydrophobic) on drug release was more noticeable in F<sub>2</sub> and F<sub>4</sub>, and the release from F<sub>2</sub> (PEO/HPC) was significantly faster than that from F<sub>4</sub> (PEO/EC) ( $f_2 = 47.53$ ).

When the formulations were thermally processed in HME and 3D printing, the pattern was reversed, and the dissolution profile followed the hydrophilic or hydrophobic nature of HPC or EC rather than the  $M_w$  of PEO (Figure 11). F<sub>1</sub> and F<sub>2</sub> (containing HPC) had a much faster release

rate than F<sub>3</sub> and F<sub>4</sub> (containing EC) in both HME and 3D-printed tablets. Moreover, F<sub>1</sub> and F<sub>2</sub> had similar release profiles, i.e.,  $f_2 = 88.08$  and  $65.28$  for HME and 3D-printed tablets, respectively, despite having different  $M_w$  of PEO. Similarly, F<sub>3</sub> and F<sub>4</sub> had similar release behavior, i.e.,  $f_2 = 83$  and  $86.45$  for HME and 3D printed tablets, respectively. This pattern was also observed in other studies, where the dissolution profiles of different  $M_w$  PEOs were relatively similar after thermal processing.<sup>1,13</sup> Based on such findings and considering GPC-proven PEO degradation in heat-processed methods, it can be suggested that after a specific degradation in the  $M_w$  of PEO, gelling behavior becomes weak, and drug release becomes less sensitive to PEO  $M_w$ . A similar pattern was also noticed in a stability study of PEO tablets, where, after eight weeks of storage at high temperatures and humidity, all  $M_w$  exhibited similar release profiles.<sup>8,9</sup>

### 3.8. Release kinetics

Dissolution kinetics were also analyzed using four kinetic models (zero-order, first-order, Higuchi, and Korsmeyer-

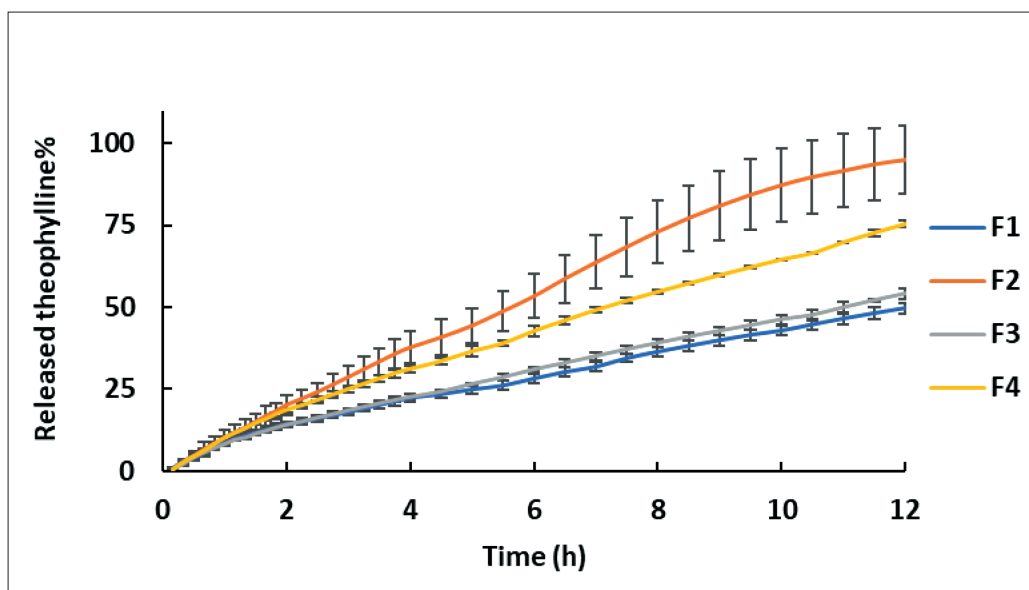


Figure 10. Comparison of dissolution behavior of the four formulations ( $F_1$ – $F_4$ ) prepared by physical mixture (PM) method.

Peppas) to investigate changes in the mechanism of drug release due to manufacturing methods. According to Table 8, the manufacturing method appears to impact the release kinetics of tablets. The drug release from PM tablets of  $F_1$  and  $F_3$  (containing high  $M_w$  PEO) fits best with the first-order mechanism ( $R^2 > 0.99$ ), while the same formulations made by HME and 3D printing best follow the Higuchi model ( $R^2 > 0.99$ ). Meanwhile,  $F_2$  and  $F_4$  tablets (containing low  $M_w$  PEO) made by the PM method follow a zero-order drug release ( $R^2 > 0.99$ ), but the release mechanism changed to Higuchi ( $R^2 \geq 0.99$ ) in HME and 3D-printed tablets.

For the release mechanism,  $n$  values from the Korsmeyer-Peppas model determine the drug release mechanism associated with each manufacturing method. All tablets displayed good fitting with the Korsmeyer-Peppas model ( $0.84 < R^2 < 0.99$ ).  $F_2$  and  $F_4$  (containing lower  $M_w$  PEO, 0.9 M) have similar release mechanisms with  $n > 0.85$ , indicating diffusion in all manufacturing methods despite significant changes in DE%. However, formulations containing PEO 7 M exhibited different patterns.  $F_1$  features an anomalous transport (diffusion and swelling) mechanism in PM tablets ( $n = 0.766$ ). However, in HME and 3D-printed tablets, the mechanism is polymer relaxation ( $n = 1.287$  and  $1.157$ , respectively).  $F_3$  also demonstrated the same pattern with  $n$ -values of 0.845, 1.282, and 0.939 for PM, HME, and printed tablets, respectively. Upon observation, PM tablets of  $F_1$  and  $F_3$  (with 7 M PEO) transformed into a thick gel ball at the end of the dissolution test, but this was absent in HME and printed tablets; this was also observed in other studies.<sup>8,9</sup> It is assumed that below a specific grade of  $M_w$ , the release

mechanism and dissolution rate can be less sensitive to  $M_w$  changes.

Considering the dissolution profiles and mechanism of drug release, it can be concluded that FDM 3D printing can produce tablets with increased hardness and porosity, but lower density and crystallinity, compared to PM and HME methods. Although porosity and density can affect the release profile, their effect can be outweighed by the effect of hardness and formulation composition. Previous work indicates that increased hardness can extend the release profile of printed tablets when a considerable amount (>40%) of hydrophobic material is included in the formulation.<sup>16,26,41</sup> However, the delayed release effect of elevated hardness can be minimized when the formulation is completely hydrophilic.<sup>16</sup> PEO, as a polymer, can suffer from degradation and  $M_w$  reduction under thermal conditions of HME and 3D printing, subsequently reducing its gelling ability to extend drug release. Its crystallinity also decreases, which can increase DE%. Thus, an increase in DE% may be observed after heat processing, such as 3D printing, as observed for  $F_1$  and  $F_2$ . Moreover, the impact of heat-induced PEO  $M_w$  reduction on drug release has its limitations. When high  $M_w$  PEO is used (7 M),  $M_w$  degradation in HME could significantly change DE% and its release mechanism, like in  $F_1$ . However, further degradation during the printing method (evidenced by GPC) displayed negligible impact on DE% or its release mechanisms. Similarly, variations in DE% of  $F_2$ , which contains a lower  $M_w$  of PEO (0.9 M), were minimal, and the release mechanism was consistent across PM, HME, and printed tablets.

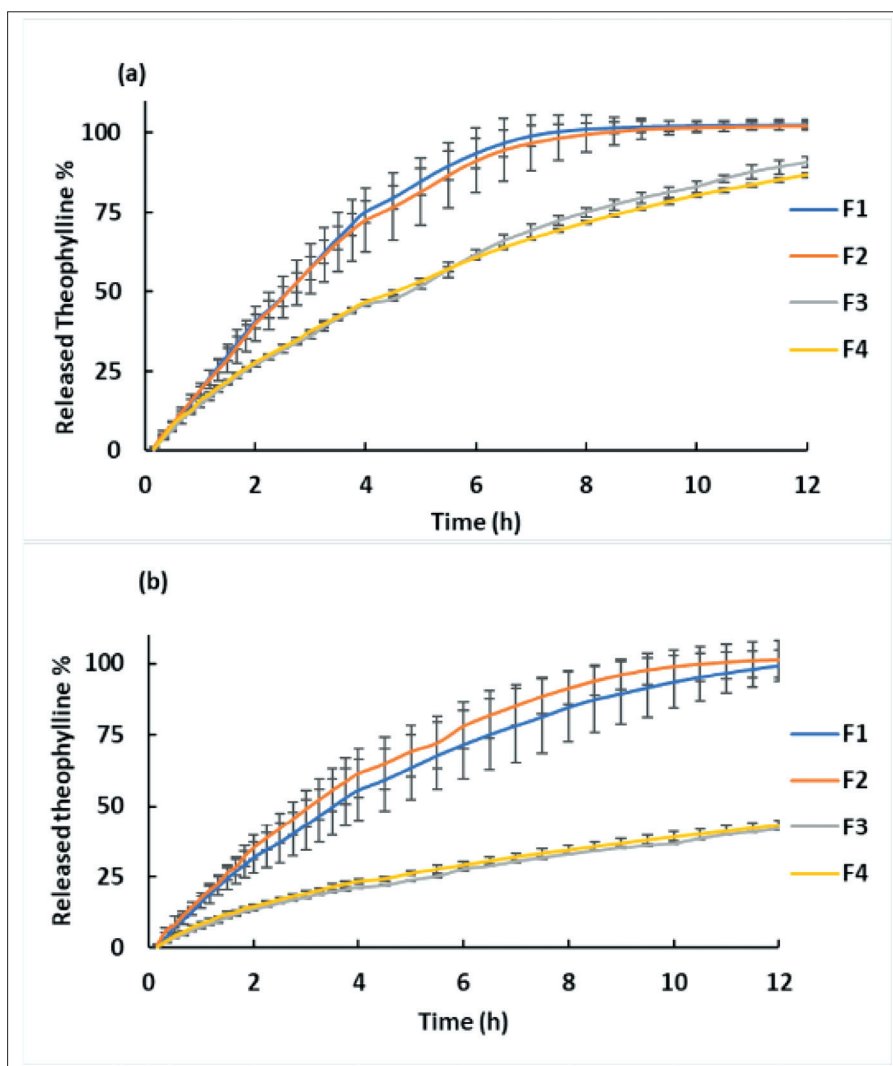


Figure 11. Comparison of dissolution behavior of the four formulations (F<sub>1</sub>-F<sub>4</sub>) prepared by the (a) hot-melt extrudate (HME) and (b) 3D-printing method.

Table 8. Kinetic parameters for F<sub>1</sub>-F<sub>4</sub> prepared as a physical mixture (PM), hot-melt extrudates (HME), and by 3D printing.

Kinetic model	Parameter	F <sub>1</sub>			F <sub>2</sub>			F <sub>3</sub>			F <sub>4</sub>		
		PM	HME	Printed	PM	HME	Printed	PM	HME	Printed	PM	HME	Printed
Zero-order	R <sup>2</sup>	0.991	0.97	0.951	0.992*	0.958	0.97	0.991	0.967	0.965	0.992*	0.957	0.957
First-order	R <sup>2</sup>	0.996*	0.859	0.939	0.901	0.875	0.877	0.997*	0.990	0.986	0.989	0.998*	0.981
Higuchi	R <sup>2</sup>	0.985	0.992*	0.994*	0.976	0.990*	0.996*	0.988	0.997*	0.999*	0.988	0.998*	1.00
Korsmeyer-Peppas	R <sup>2</sup>	0.979	0.98	0.976	0.976	0.990*	0.969	0.959	0.845	0.877	0.939	0.935	0.869
	n	0.77	1.29	1.16	1.05	1.17	1.03	0.85	1.28	0.94	1.02	1.04	0.90

Note: \*denotes Highest value of R<sup>2</sup>. Abbreviations: PM: Physical mixture; HME: Hot-melt extrudate.



#### 4. Conclusion

Two high  $M_w$  PEOs (7 M and 0.9 M) were used to produce extended-release tablets using direct compression of a PM of the formulation constituents or thermal processing of these mixtures via HME and FDM 3D printing. The studied formulations contained PEO mixed with theophylline (drug) and another polymer (HPC or EC). GPC studies demonstrated that PEO undergoes  $M_w$  reduction after thermal and mechanical stress in HME and FDM 3D printing, while XRPD displayed a reduction in crystallinity. These physical changes reduced the gelling behavior of PEO, resulting in faster drug release, which was more significant with higher  $M_w$  PEOs. As expected, HME and printed tablets exhibited significantly increased drug release compared to PM tablets. Conversely, the inclusion of hydrophobic materials in the formulation outweighs the impact of PEO degradation in 3D printing, leading to extended drug release. These hydrophobic polymers (like EC) are beneficial as they prevent the disintegration of tablets during dissolution and provide more control over dissolution behavior. Our findings and those of other studies suggest that printing methods appear to be more effective in extending drug release when hydrophobic materials are used. However, PEO remains a viable option for 3D printing, though it demands stringent process control to ensure consistent drug release and desired physicochemical properties.

#### Acknowledgments

None.

#### Funding

This research received no external funding.

#### Conflict of interest

The authors declare they have no competing interests.

#### Author contributions

**Conceptualization:** Matthew Lam, Taravat Ghafourian, Ali Nokhodchi

**Formal analysis:** Nour Nashed, Ali Nokhodchi, Taravat Ghafourian

**Investigation:** Nour Nashed, Mridul Majumder, Barnaby W. Greenland

**Methodology:** Nour Nashed, Barnaby W. Greenland, Mridul Majumder

**Writing – original draft:** Nour Nashed

**Writing – review & editing:** Matthew Lam, Taravat Ghafourian, Ali Nokhodchi

#### Ethics approval and consent to participate

Not applicable.

#### Consent for publication

Not applicable.

#### Availability of data

Data used in this study are available from the corresponding author upon reasonable request.

#### References

1. Salem S, Byrn SR, Smith DT, et al. Impact assessment of the variables affecting the drug release and extraction of polyethylene oxide based tablets. *J Drug Deliv Sci Technol.* 2022;71:103337. doi: 10.1016/j.jddst.2022.103337
2. Meruva S, Donovan MD. Polyethylene oxide (PEO) molecular weight effects on abuse-deterrent properties of matrix tablets. *AAPS PharmSciTech.* 2020;21:1-10. doi: 10.1208/s12249-019-1565-y
3. Pajander J, Rensonnet A, Hietala S, et al. The evaluation of physical properties of injection molded systems based on poly(ethylene oxide) (PEO). *Int J Pharm.* 2017;518(1-2):203-212. doi: 10.1016/j.ijpharm. 2016.12.050
4. Maggi L, Bruni R, Conte U. High molecular weight polyethylene oxides (PEOs) as an alternative to HPMC in controlled release dosage forms. *Int J Pharm.* 2000;195(1-2):229-238. doi: 10.1016/S0378-5173(99)00402-0
5. Malik P, Castro M, Carrot C. Thermal degradation during melt processing of poly(ethylene oxide), poly(vinylidene fluoride-co-hexafluoropropylene) and their blends in the presence of additives, for conducting applications. *Polym Degrad Stab.* 2006;91(4):634-640. doi: 10.1016/j.polymdegradstab.2005.01.020
6. Crowley MM, Zhang F, Koleng JJ, et al. Stability of polyethylene oxide in matrix tablets prepared by hot-melt extrusion. *Biomaterials.* 2002;23(21):4241-428. doi: 10.1016/S0142-9612(02)00187-4
7. Cantin O. *PEO Hot Melt Extrudates for Controlled Drug Delivery* (Doctoral dissertation, Université du Droit et de la Santé–Lille II). 2017. <https://tel.archives-ouvertes.fr/tel-01540630>
8. Shojaee S, Asare-Addo K, Kaialy W, et al. An investigation into the stabilization of diltiazem HCl release from matrices made from aged polyox powders. *AAPS PharmSciTech.* 2013;14(3):1190-1198. doi: 10.1208/s12249-013-0013-7

9. Shojaee S, Cumming I, Kaialy W, et al. The influence of vitamin E succinate on the stability of polyethylene oxide PEO controlled release matrix tablets. *Colloids Surf B Biointerfaces*. 2013;111:486-492. doi: 10.1016/j.colsurfb.2013.06.038
10. Vrandečić NS, Erceg M, Jakić M, et al. Kinetic analysis of thermal degradation of poly(ethylene glycol) and poly(ethylene oxide)s of different molecular weight. *Thermochim Acta*. 2010;498(1-2):71-80. doi: 10.1016/j.tca.2009.10.005
11. Smith KL, Van Cleve R. High molecular weight polymers of ethylene oxide plastic properties. *Indus Eng Chem*. 1958;50(1):12-16. doi: 10.1021/ie50577a024
12. Repka MA, McGinity JW. Influence of vitamin E TPGS on the properties of hydrophilic films produced by hot-melt extrusion. *Int J Pharm*. 2000;202(1-2):63-70. doi: 10.1016/S0378-5173(00)00418-X
13. Cantin O, Siepmann F, Danede F, et al. PEO hot melt extrudates for controlled drug delivery: importance of the molecular weight. *J Drug Deliv Sci Technol*. 2016;36:130-140. doi: 10.1016/j.jddst.2016.09.003
14. Isreb A, Baj K, Wojsz M, et al. 3D printed oral theophylline doses with innovative 'radiator-like' design: impact of polyethylene oxide (PEO) molecular weight. *Int J Pharm*. 2019;564:98-105. doi: 10.1016/j.ijpharm.2019.04.017
15. Ong JJ, Awad A, Martorana A, et al. 3D printed opioid medicines with alcohol-resistant and abuse-deterrent properties. *Int J Pharm*. 2020;579:119169. doi: 10.1016/j.ijpharm.2020.119169
16. Nashed N, Lam M, Ghafourian T, et al. An insight into the impact of thermal process on dissolution profile and physical characteristics of theophylline tablets made through 3D printing compared to conventional methods. *Biomedicines*. 2022;10(6):1-18. doi: 10.3390/biomedicines10061335
17. Quinten T. Evaluation of injection molding as a pharmaceutical production technology for sustained-release matrix tablets. *Ghent University*. 2010. <http://library1.nida.ac.th/termpaper6/sd/2554/19755.pdf>
18. Shodexhplc, Poly (Ethylene Oxide) Standards. Available from: [shodexhplc.com/applications/poly-ethylene-oxide-standards/](http://shodexhplc.com/applications/poly-ethylene-oxide-standards/)
19. Stringano E, Gea A, Salminen JP, et al. Simple solution for a complex problem: proanthocyanidins, galloyl glucoses and ellagitannins fit on a single calibration curve in high performance-gel permeation chromatography. *J Chromatogr A*. 2011;1218(43):7804-7812. doi: 10.1016/j.chroma.2011.08.082
20. Dishman KL. Sieving in particle size analysis. In: *Encyclopedia of Analytical Chemistry*. Wiley; 2000. doi: 10.1002/9780470027318.a1514.
21. Tan DK, Maniruzzaman M, Nokhodchi A. Development and optimisation of novel polymeric compositions for sustained release theophylline caplets (PrintCap) via FDM 3D printing. *Polymers*. 2020;12(1):1-18. doi: 10.3390/polym12010027
22. Anderson NH, Bauer M, Boussac N, et al. An evaluation of fit factors and dissolution efficiency for the comparison of *in vitro* dissolution profiles. *J Pharm Biomed Anal*. 1998;17(4-5):811-822. doi: 10.1016/S0731-7085(98)00011-9
23. Zhang Y, Huo M, Zhou J, et al. DDSolver: an add-in program for modeling and comparison of drug dissolution profiles. *AAPS J*. 2010;12(3):263-271. doi: 10.1208/s12248-010-9185-1
24. Ritger PL, Peppas NA. A simple equation for description of solute release I. Fickian and non-fickian release from non-swelling devices in the form of slabs, spheres, cylinders or discs. *J Control Release*. 1987;5(1):23-36. doi: 10.1016/0168-3659(87)90034-4
25. Bruschi ML. Mathematical models of drug release. In: *Strategies to Modify the Drug Release from Pharmaceutical Systems*. Sawston, UK: Woodhead Publishing; 2015:63-86. doi: 10.1016/B978-0-08-100092-2.00005-9
26. Shi K, Slavage JP, Maniruzzaman M, et al. Role of release modifiers to modulate drug release from fused deposition modelling (FDM) 3D printed tablets. *Int J Pharm*. 2021;597:120315. doi: 10.1016/j.ijpharm.2021.120315
27. Ashland Inc. Klucel Hydroxypropylcellulose Physical and Chemical Properties (Datasheet). 2017. [http://www.ashland.com/file\\_source/Ashland/Product/Documents/Pharmaceutical/PC\\_11229\\_Klucel\\_HPC.pdf](http://www.ashland.com/file_source/Ashland/Product/Documents/Pharmaceutical/PC_11229_Klucel_HPC.pdf)
28. Homae Borujeni S, Mirdamadian SZ, Varshosaz J, et al. Three-dimensional (3D) printed tablets using ethyl cellulose and hydroxypropyl cellulose to achieve zero order sustained release profile. *Cellulose*. 2020;27(3):1573-1589. doi: 10.1007/s10570-019-02881-4
29. Polaskova M, Peer P, Cermak R, et al. Effect of thermal treatment on crystallinity of poly(ethylene oxide) electrospun fibers. *Polymers*. 2019;11(9):1384. doi: 10.3390/polym11091384
30. PerkinElmer. Polymer crystallinity studies by DSC- Raman spectroscopy. 2009. <https://perkinelmer.cl/wp-content/uploads/2018/05/Polymer-Crystallinity-by-DSC-Raman.pdf>
31. Park MS, Kim JK. Phase behavior and crystallization of a poly(ethylene oxide)/cellulose acetate butyrate blend. *J Polym Sci B Polym Phys*. 2002;40(15):1673-1681.

- doi: 10.1002/polb.10225
32. Leineweber A. Reflection splitting-induced microstrain broadening. *Powder Diffraction*. 2017;32(S1):S35-S39. doi: 10.1017/S0885715617000665
33. Bhagia S, Gallego NC, Hiremath N, et al. Fine grinding of thermoplastics by high speed friction grinding assisted by guar gum. *J Appl Polym Sci*. 2021;138(32):50797. doi: 10.1002/app.50797
34. Schmidt J, Plata M, Tröger S, et al. Production of polymer particles below 5µm by wet grinding. *Powder Technol*. 2012;228:84-90. doi: 10.1016/j.powtec.2012.04.064.
35. Jung H, Lee YJ, Yoon WB. Effect of moisture content on the grinding process and powder properties in food: a review. *Processes*. 2018;6(6):69. doi: 10.3390/pr6060069
36. Eckert A, Abbasi M, Mang T, et al. Structure, mechanical properties, and dynamics of polyethylenoxide/nanoclay nacre-mimetic nanocomposites. *Macromolecules*. 2020;53(5):1716-1725. doi: 10.1021/acs.macromol.9b01931
37. Xiao P, Guo Y, Wang J, et al. The effect of granules characters on mechanical properties of press-coated tablets: a comparative study. *Int J Pharm*. 2022;624:121986. doi: 10.1016/j.ijpharm.2022.121986
38. Vinayagamoorthy R. Effect of particle sizes on the mechanical behaviour of limestone-reinforced hybrid plastics. *Polym Polym Compos*. 2020;28(6):410-420. doi: 10.1177/0967391119883163
39. Huang Y, Paul DR. Effect of temperature on physical aging of thin glassy polymer films. *Macromolecules*. 2005;38(24):10148-1054. doi: 10.1021/ma051284g
40. Greiner R, Schwarzl FR. Volume relaxation and physical aging of amorphous polymers I. theory of volume relaxation after single temperature jumps. *Colloid Polym Sci*. 1989;267(1):39-47. doi: 10.1007/BF01410147
41. Zhang J, Feng X, Patil H, et al. Coupling 3D printing with hot-melt extrusion to produce controlled-release tablets. *Int J Pharm*. 2016;519:186-197. doi: 10.1016/j.ijpharm.2016.12.049